The Astrophysical Journal Letters, 745:L18 (6pp), 2012 February 1 doi:10.1088/2041-8205/745/2/L18

FIRST SIMULTANEOUS OBSERVATION OF AN Hα MORETON WAVE, EUV WAVE, AND FILAMENT/PROMINENCE OSCILLATIONS

Ayumi Asai[1], Takako T. Ishii[2], Hiroaki Isobe[1], Reizaburo Kitai[2], Kiyoshi Ichimoto[2], Satoru UeNo[2], Shin'ichi Nagata[2], Satoshi Morita[2], Keisuke Nishida[2], Daikou Shiota[3], Akihito Oi[4], Maki Akioka[5], and Kazunari Shibata[2]
[1] Unit of Synergetic Studies for Space, Kyoto University, Yamashina, Kyoto 607-8471, Japan; asai@kwasan.kyoto-u.ac.jp
[2] Kwasan and Hida Observatories, Kyoto University, Yamashina, Kyoto 607-8471, Japan
[3] Advanced Science Institute, RIKEN, Wako, Saitama 351-0198, Japan
[4] College of Science, Ibaraki University, Mito, Ibaraki 310-8512, Japan
[5] Hiraiso Solar Observatory, National Institute of Information and Communications Technology, Hitachinaka, Ibaraki 311-1202, Japan
Received 2011 October 4; accepted 2011 December 26; published 2012 January 6

ABSTRACT

We report on the first simultaneous observation of an Hα Moreton wave, the corresponding EUV fast coronal waves, and a slow and bright EUV wave (typical EIT wave). We observed a Moreton wave, associated with an X6.9 flare that occurred on 2011 August 9 at the active region NOAA 11263, in the Hα images taken by the Solar Magnetic Activity Research Telescope at Hida Observatory of Kyoto University. In the EUV images obtained by the Atmospheric Imaging Assembly on board the *Solar Dynamic Observatory* we found not only the corresponding EUV fast "bright" coronal wave, but also the EUV fast "faint" wave that is not associated with the Hα Moreton wave. We also found a slow EUV wave, which corresponds to a typical EIT wave. Furthermore, we observed, for the first time, the oscillations of a prominence and a filament, simultaneously, both in the Hα and EUV images. To trigger the oscillations by the flare-associated coronal disturbance, we expect a coronal wave as fast as the fast-mode MHD wave with the velocity of about 570–800 km s^{-1}. These velocities are consistent with those of the observed Moreton wave and the EUV fast coronal wave.

Key words: magnetohydrodynamics (MHD) – shock waves – Sun: corona – Sun: filaments, prominences – Sun: flares

1. INTRODUCTION

Moreton waves, flare-associated waves seen in Hα, have been observed (Moreton 1960; Smith & Harvey 1971; Shibata et al. 2011) to propagate in restricted angles with the velocity of about 500–1500 km s^{-1}. They sometimes show arc-shaped fronts and are often associated with type-II radio bursts (Kai 1970). They are transient and appear only for about 10 minutes. Associated with flares, remote filaments and prominence are sometimes activated or excited to oscillate. These "winking filaments" are also thought to be caused by flare-associated waves and are called as invisible Moreton waves (Smith & Harvey 1971; Tripathi et al. 2009; Hershaw et al. 2011). After the findings, Uchida (1968) suggested that Moreton waves are the intersection of the fast-mode magnetohydrodynamic (MHD) shock propagating in the corona with chromosphere. This model has been widely accepted, and the coronal counterparts have been surveyed for a few decades. Moreton waves are rarely observed even for large flares (Shibata et al. 2011).

After the launch of the *Solar and Heliospheric Observatory*, the EUV Imaging Telescope (EIT) found wave-like phenomena associated with flares, which are called "EIT waves" (Thompson et al. 1999, 2000). Although EIT waves were expected to be the coronal counterpart of Moreton waves, they show physical characteristics different from those of Moreton waves: the propagating velocity is much slower than that of the Moreton wave and is about 200–400 km s^{-1}, the lifetime is much longer and is about 45–60 minutes, and they can show isotropic propagation, while Moreton waves propagate with restricted angles (Klassen et al. 2000; Warmuth 2007; Thompson & Myers 2009). Therefore, there remained a question whether EIT waves are really coronal counterparts of Moreton waves or not. As for searching a coronal counterpart of Moreton waves, the Soft X-ray Telescope on board *Yohkoh* found wave-like phenomena in soft X-rays, called X-ray waves (Khan & Hudson 2000; Khan & Aurass 2002). X-ray waves are confirmed to be a real counterpart of Moreton waves by simultaneous observations of X-ray waves and Moreton waves (Narukage et al. 2002, 2004).

Then, we come to the issue of what EIT waves are. Eto et al. (2002) clearly showed that an EIT wave is different from a Moreton wave, based on their simultaneous observations. On the other hand, Warmuth et al. (2004a, 2004b) argue that the velocity discrepancy of the EIT and Moreton waves can be explained by the deceleration of coronal waves. The mechanism of EIT waves remains, therefore, very controversial (Warmuth 2007; Wills-Davey & Attrill 2009; Gallagher & Long 2010). Delannée & Aulanier (1999) and Chen et al. (2002, 2005) proposed the field-line stretching model for EIT waves. They suggested that EIT bright fronts were not "waves" at all, but instead plasma compression at stable flux boundaries due to rapid magnetic field expansion. This model can also resolve the puzzle of why EIT waves often stop at magnetic separatrices.

Recently, fast coronal waves have been observed to be associated with flares (e.g., Liu et al. 2010; Ma et al. 2011) by the Atmospheric Imaging Assembly (AIA; Title & AIA Team 2006; Lemen et al. 2011) on board the *Solar Dynamic Observatory* (*SDO*). These waves (hereafter called "EUV fast coronal waves") are thought to be fast-mode MHD waves. Coronal X-ray waves and EUV fast coronal waves have also been observed spectroscopically with the EUV Imaging Spectrometer (EIS) on board *Hinode* (Asai et al. 2008; Harra et al. 2011).

Chen & Wu (2011) found two different co-existing coronal waves, a slow coronal wave (i.e., EIT wave) and a fast coronal wave, from EUV observations taken by *SDO*/AIA. Although the fast coronal wave seems to be the coronal counterpart of a Moreton wave, they used only EUV images, and it remained to

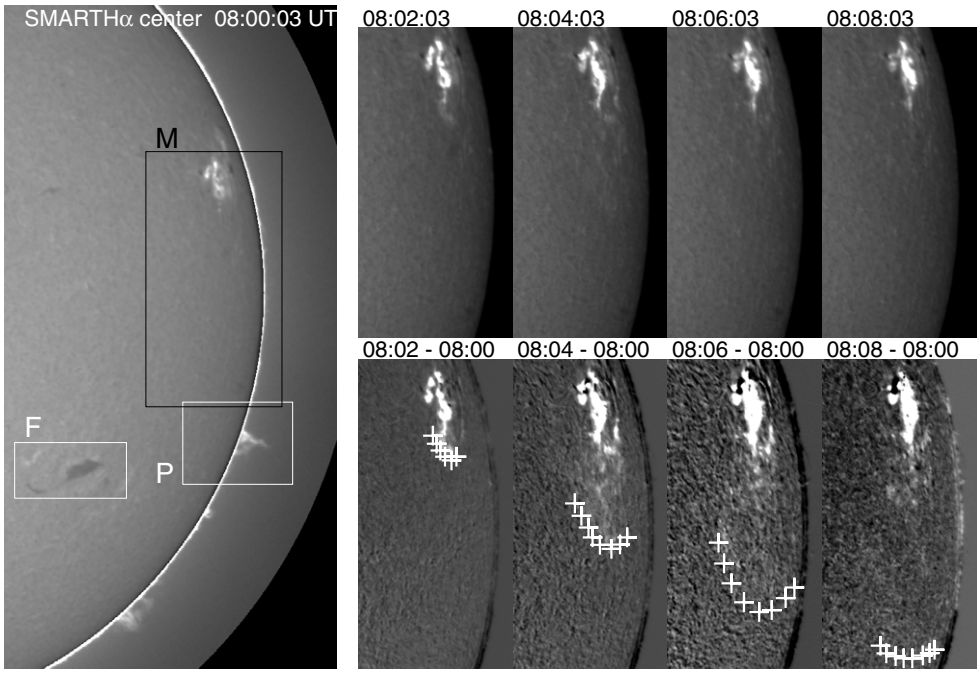

Figure 1. Propagation of the Moreton wave observed with SMART. Solar north is up and west to the right. The top right panels are the sequence of Hα images of the region "M" (the black rectangle) in the left panel. The bottom right panels are the same sequence of the Hα images but are subtracted with the image at 08:00 UT. The white rectangles with marks "P" and "F" in the left panel indicate the oscillating prominence and filament, respectively.

be confirmed whether it is a classical Hα Moreton wave. This Letter presents the first simultaneous observation of EUV waves and a Moreton wave by using EUV and Hα images with high spatial and temporal resolutions. Moreover, we found not only a winking filament on the disk, but also an oscillating prominence on the limb, triggered by the coronal wave (Moreton wave).

2. OBSERVATIONS

An intense flare, X6.9 on the *GOES* scale, occurred on 2011 August 9 at the Active Region NOAA 11263 (17°N, 71°W). The flare started at 07:48 UT and peaked at 08:05 UT. We observed a Moreton wave associated with the flare in the Hα images obtained by the Solar Magnetic Activity Research Telescope (SMART; UeNo et al. 2004) at Hida Observatory, Kyoto University, Japan. SMART regularly observes the full-disk Sun in seven wavelengths around the Hα line (6562.8 Å), i.e., Hα center and the wings at $\pm$0.5, $\pm$0.8, and $\pm$1.2 Å. The time cadence is 2 minutes for each wavelength during the impulsive phase of the flare, and the pixel size is 0.″56. Such full-disk and multi-wavelength observation with high cadence is suitable to detect Moreton waves (e.g., Narukage et al. 2008). The Moreton wave was seen only from 08:02 UT to 08:08 UT with the SMART data. Figure 1 shows the Moreton wave in Hα center images taken by SMART. It mainly traveled southward from the flare site. We derived the propagation speed by following the fastest wavefront. The mean propagation speed during the 6 minute appearance of the Moreton wave was about 760 km s^{-1}. The Hα $-$1.2 Å images taken with SMART show the ejection of a filament with the velocity of about 300 km s^{-1} in the direction of the Moreton wave.[6]

To compare the physical features of Hα Moreton waves with wave-like phenomena observed in EUVs, we used EUV images taken by *SDO*/AIA. In this Letter we mainly used the 193 Å images, which are mainly attributed to the Fe XII ($\log(T) \sim 6.1$) line. The temporal resolution of the AIA 193 Å data during the flare was 12 s. The flare site was close to the west limb. We also used EUV images taken by the Extreme-Ultraviolet Imager (EUVI) of the Sun–Earth Connection Corona and Heliospheric Investigation (SECCHI; Howard et al. 2008) on board the *Solar Terrestrial Relations Observatory* (*STEREO*; Kaiser et al. 2008) *Ahead* satellite (*STEREO-A*). *STEREO-A* was ∼100.°7 ahead of the Earth at the time of the flare. The temporal resolutions of the 195 and 304 Å data, which we used in this Letter, were 5 and 10 minutes, respectively. The pixel size of the images is 1.″58.

Figure 2 shows the wave propagation seen in the *SDO*/AIA 193 Å images (top) and in the *STEREO-A*/EUVI 195 Å images (bottom). All are difference images, and are subtracted by the intensity maps taken at 07:55:19 and 07:55:31 UT for AIA and EUV data, respectively. The right panels of Figure 2 show the potential magnetic field lines for the view from the Earth (top) and from *STEREO-A* (bottom). The potential magnetic field lines are calculated by using synoptic magnetograms from GONG data[7] and based on the method by Shiota et al. (2008). In the images at 08:05 UT we can identify sharp wavefronts traveling southward, similar to that reported by Thompson et al. (2000), while the sharp fronts disappear after 08:10 UT. The EIT wave was blocked by small ARs from traveling and did not show the isotropic feature. The magnetic field of the southern region of the flare site is weak. A part of the EUV wave traveling southward, which is shown with the arrows in Figure 2, traveled without being disturbed by such ARs. The propagation velocity of about 700 km s^{-1} was measured by following the wavefronts in the images. The wavefront is much fainter than the sharp front seen at 08:05 UT.

3. ANALYSIS AND RESULTS

In Figures 3(a) and (b), we show the comparison of the spatial structure of the Moreton wave with that of the EUV wave of this

[6] See http://www.kwasan.kyoto-u.ac.jp/topics/110809/bin_p12/.

[7] http://gong.nso.edu/data/magmap/

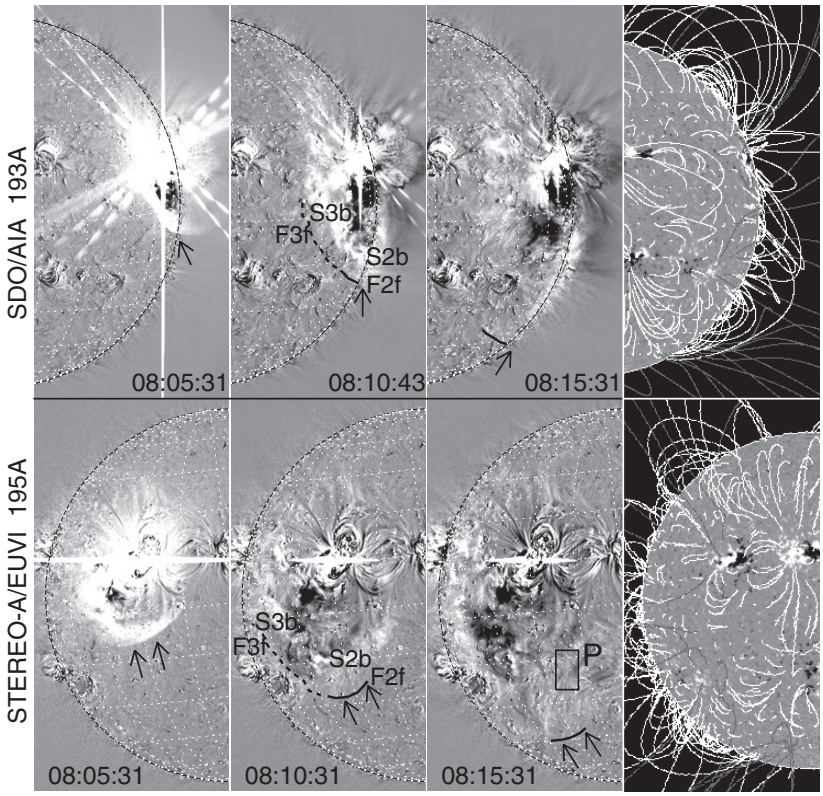

Figure 2. EUV waves observed with *SDO*/AIA 193 Å (top) and *STEREO-A*/SECCHI/EUVI 195 Å (bottom). The arrows follow the front of the EUV fast coronal wave. The region with mark P points to the position of the limb prominence. The right panels show the potential magnetic field lines for the views from the Earth (top right) and from *STEREO-A* (bottom right).

flare. These are the difference images in AIA 193 Å and in the SMART Hα center, respectively. The time difference is noted in the figure. The plus (+) signs follow the front of the Moreton wave. The front is well coincident with the sharp bright EUV wavefront. In addition, we can identify an expanding dome on the wavefront in AIA EUV images. Therefore, the expanding dome is thought to be the shock traveling in the corona, and the Moreton wave and the sharp EUV wave are the intersection with the chromosphere.

We examined the temporal features of the EUV wave by using the time–distance diagrams (time-slice images) along the lines shown in Figure 3(a). Figures 3(c), (d), and (e) are the time-slice images for Lines 1, 2, and 3, respectively. For each diagram, the flare site was set to be zero. The velocities were derived by following the features in the time-slice diagrams. Line 1, which is drawn with a straight line, mainly follows the dome structure expanding in the corona. In the time-slice images (Figure 3(c)), we can see a bright front (F1) with traveling velocity of about 760 km s^{-1}, though initially it is even faster. Behind the front, we can identify the dimming feature. Line 2 mainly follows the same path of the Moreton wave and is following the great circle of the solar surface from the flare site. The front is very bright and sharp from 08:01 to 08:09 UT (F2b), which is almost the same time range as the Moreton wave. Even after 08:09 UT, we can identify the wavefront, though it became much fainter (F2f). The traveling velocities are about 730 and 620 km s^{-1} for F2b and F2f, respectively. On the other hand, the bright edge is rapidly decelerated (S2b) and disappears at 08:12 UT. We also draw Line 3, which also follows the great circle of the solar surface. Although the direction of Line 3 is out of the arc of the Moreton wavefront, we can see a wave-like feature. The propagation velocity of the bright front is initially about 550 km s^{-1} (F3b) and slows down to about 340 km s^{-1} (S3b) after 08:06 UT. The slow-bright EUV wave (S3b) suddenly disappears at about 08:12 UT. On the other hand, we can identify a fast-faint feature (F3f) from 08:06 UT. The velocity is about 580 km s^{-1}. As we mentioned above, there are small ARs on the passes of the EUV waves. These small closed loops start oscillating due to the propagation of the coronal wave. Along Lines 2 and 3, we can identify some oscillations as shown by the white arrows in Figures 3(d) and (e).

Associated with the flare, we observed the oscillations of a prominence on the west limb and a filament on the disk. The sites of the prominence/filament are shown in the left panel of Figure 1, with the characters P (prominence) and F (filament). In Figure 4, we show the temporal evolution of the limb prominence (P) in Hα and in EUV (193 Å) taken by SMART and AIA. From the SMART Hα wing data, we can clearly see the prominence moving in the line of sight. First, the prominence became bright in the plus wing. The initial sign of the oscillation is identified with the darkening of the prominence in the −0.5 Å image taken at 08:11:57 UT. In the sequence of 08:14 UT (at least, a part of) the prominence is the brightest in the most redward wing image of the observation, i.e., +1.2 Å image (08:14:24 UT). This means that the prominence is moving away with a Doppler velocity of about 50 km s^{-1} or even faster. Then, the motion of the prominence turned blueward, and in the sequence of 08:22 UT, it is the brightest in the −1.2 Å images (08:21:45 UT). The oscillation period is roughly 15 minutes. In the AIA EUV images, on the other hand, we can also see the motion in the plane. First, it moves southward (downward in the images), then moves northward (upward) after 08:17 UT. The oscillation period is about 12–16 minutes, and the amplitude is about 10,000 km. The apparent

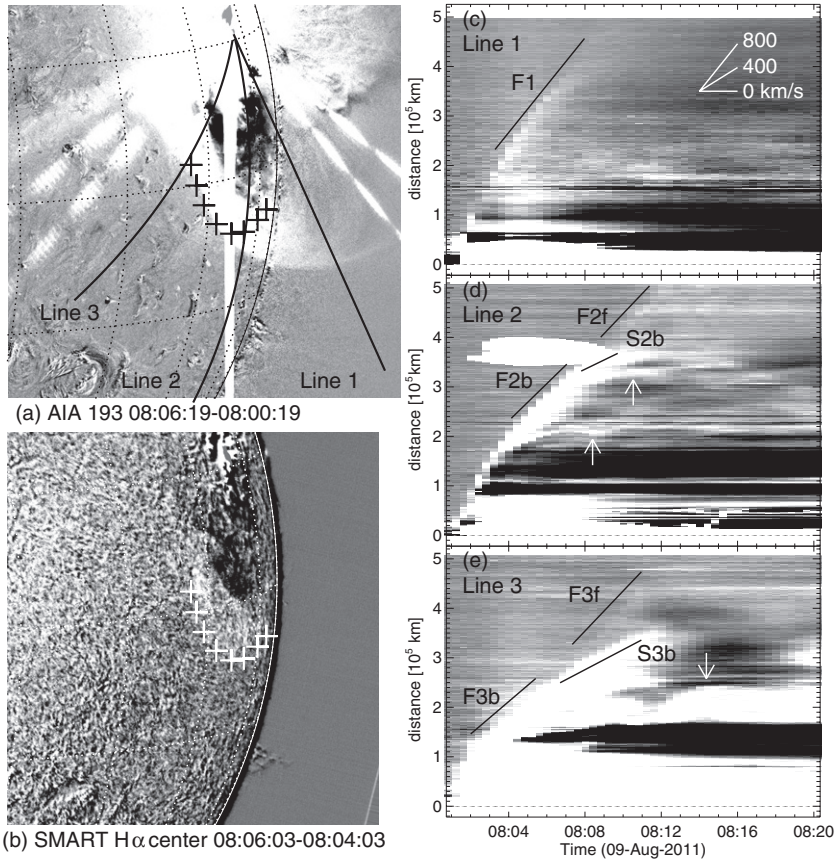

Figure 3. Detailed feature of coronal disturbances. (a) A difference image (08:06:19 − 08:00:19 UT) of EUV 193 Å image taken by *SDO*/AIA, and (b) a difference image (08:06:03 − 08:04:03 UT) of Hα center image taken by SMART. The plus (+) signs follow the Moreton wavefront. (c)–(e) Time–distance diagrams (time-slice images) of the AIA EUV 193 Å image along Lines 1, 2, and 3, respectively. The lines are shown in panel (a). The solid lines marked with F1, F2b, F2f, F3b, F3f, and S3b follow EUV wavefronts: F (fast) or S (slow), the number of the line, and b (bright) or f (faint). The white arrows point to the oscillating features caused during the propagation of the EUV waves.

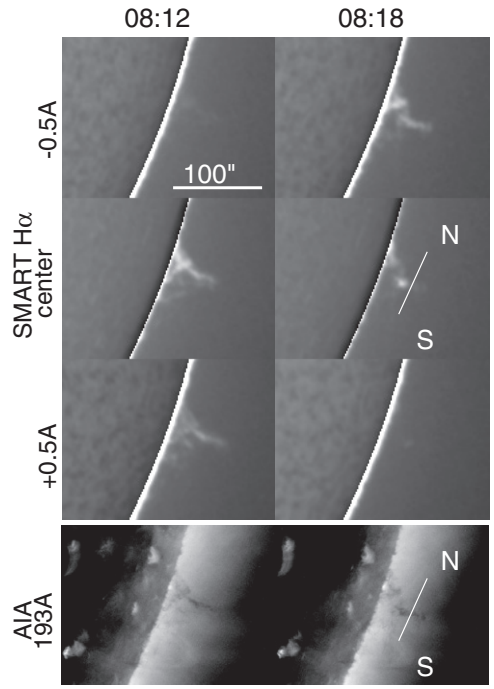

Figure 4. Temporal evolution of the oscillating prominence. From top to bottom: Hα −0.5 Å, center images, and +0.5 Å images taken by SMART, and EUV 193 Å images taken by *SDO*/AIA. The field of view of each panels is the region P shown in Figure 1. The times (UT) are indicated on the top.

velocity is about 30 km s^{-1}. In Figure 5(a), we show the time-slice image of the oscillating prominence in EUV (193 Å) overlaid with the brightest points of the prominence in the Hα center images (the plot of the + sings). The slit position is shown in Figure 4. The prominence oscillation is identified as a filament oscillation in the *STEREO-A*/EUVI 304 Å images, and we used the images to determine the precise distance from the flare site. From the start time of the oscillation and the site of the prominence, the coronal wave propagating with the velocity of about 800 km s^{-1} is expected to activate the prominence.

The filament on the disk F also showed oscillation features, although the features are much weaker both in the line-of-sight direction and in the plane than those for the prominence P. The start of the oscillation is roughly estimated as 08:17:57 UT from the Hα wing images. The oscillation period is about 15 minutes. We have to note that we can identify small activation at the footpoints of the filament F at 08:01:31 UT. Therefore, some weak movements of the filament already started when the coronal disturbance arrived at the filament. From the start time of the oscillation and the site of the filament, we expect the coronal wave to be propagating with the velocity of about 570 km s^{-1}.

4. SUMMARY AND CONCLUSIONS

We simultaneously observed the Hα Moreton wave and the corresponding EUV fast coronal wave. The Moreton wavefront

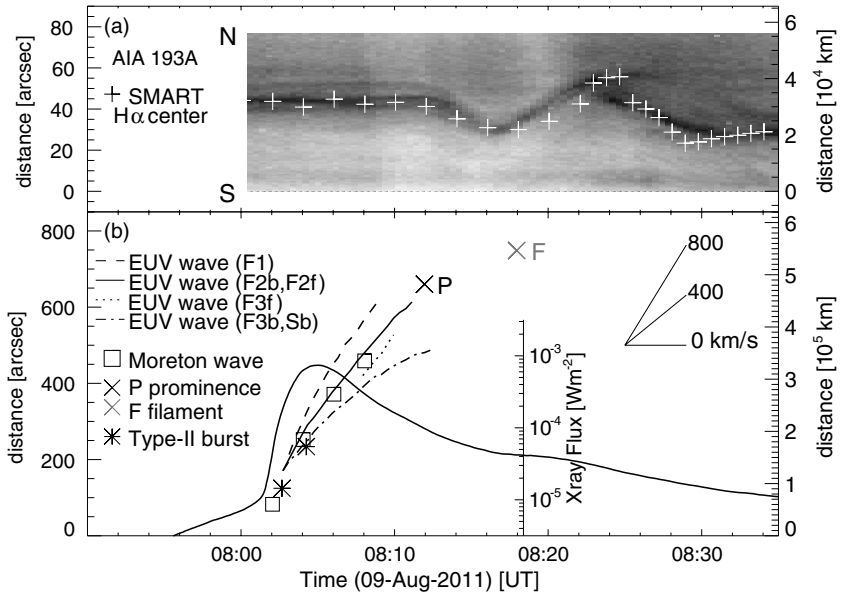

Figure 5. Height–time evolution of the flare-related phenomena. (a) A time–distance diagram (time-slice image) of the AIA EUV 193 Å image along the slit line shown in Figure 4. N and S show the north and south directions, respectively. The brightest points of the prominence in the Hα center images are overlaid with the plus (+) signs. (b) Temporal evolutions of the EUV waves, the Moreton wave, and the type-II radio burst with *GOES* X-ray flux at the 1–8 Å channel. The distance of the Moreton wavefront (□) was measured along the great circle of the solar surface from the flare site. The EUV wavefronts measured with Lines 1, 2, and 3 (see Figure 3) are shown with the dashed, solid, and dash-dotted lines, respectively. The fast-faint EUV wave seen in Line 3 (F3f) is also shown with the dotted line. The times and distances of the oscillating limb prominence (P) and disk filament (F) are shown with the cross ($\times$) signs. The distance of the type-II radio burst ($*$) was calculated by using a coronal electron density model, and the zero was set to be the photosphere.

was well consistent with the fast-bright-sharp EUV wavefront (F2b). Even after the Moreton wave disappeared, we identified the propagation of the fast-faint EUV wave (F2f). Even along Line 3 (Figure 3(a)), which is the direction without the Moreton wave, we found fast EUV waves (F3b, F3f). The fast EUV waves (F1, F2f, F3b, and F3f) are thought to be the fast-mode MHD waves (coronal waves). The EUV fast coronal waves appear more frequently than Moreton waves, although they are very faint and have not been observed until the launch of *SDO*. Specifically, only when the shock contacts the chromosphere strongly is the intersection observed as the Moreton wave (F2b). The temporal evolutions of the Hα Moreton wave and the EUV waves are summarized in Figure 5(b).

In Figure 5, we also show the temporal evolutions of a type-II radio burst associated with the flare. In the metric radio spectrogram (25–2500 MHz) observed with the Hiraiso Radio Spectrograph (HiRAS; Kondo et al. 1995), we identify the type-II radio burst from 08:02:40 to 08:06:30 UT. Assuming the coronal density model proposed by Newkirk (1961) and Mann et al. (1999), we derived the propagation velocity of about 850 km s^{-1}. The observed type-II radio burst seems to be consistent with the Moreton wave and fast-bright EUV wave, which also supports the interpretation of the wave as a fast-mode MHD shock.

We also found oscillations of a prominence and a filament. To trigger the oscillations by a flare-associated coronal disturbance, we expect a coronal wave as fast as the fast-mode MHD wave with the velocity of about 570–800 km s^{-1}. These velocities are consistent with the propagation velocities of the observed Moreton wave and the EUV fast coronal wave. An invisible Moreton wave could be such an EUV fast-faint coronal wave. It is known that a typical slow EIT wave sometimes causes filament oscillations (Okamoto et al. 2004), or such filament oscillations triggered by an EIT wave are expected to be stronger than those by an invisible Moreton wave (P. F. Chen 2011, private communication). In the current case, however, the role of the EIT wave on the filament/prominence oscillations is unclear.

Along Lines 2 and 3, we identified slow-bright EUV waves (S2b, S3b) behind the fast-faint EUV waves. From the propagating features (i.e., the velocity and the isotropic propagation; Figure 2), we think it is a typical EIT wave. We simultaneously observed the EIT wave and the EUV fast wave (fast-mode MHD wave) as reported by Chen & Wu (2011). This means that the EIT wave is different from a fast-mode MHD wave, which supports the field-line stretching model (Chen et al. 2002, 2005). It is, however, difficult to clearly identify both features separately in the very initial phase of the flare, and the relation between the fast-bright (F3f) and the slow-bright (S3b) EUV waves along Line 3 is unclear.

There is the alternative possibility that we observed a single coronal disturbance, and that two different waves (F2f/F3f and S2b/S3b) correspond to the fronts of two different heights (faster ones are higher) of the disturbance (Veronig et al. 2008; Warmuth & Mann 2011).

We, however, do not think this is possible due to the following reasons. First, the slow-bright waves (S2b, S3b) stopped propagating at small active regions. This conflicts with the features of a fast-mode wave, though this is possibly reconciled by considering the stopping front as CME flanks as reported by Patsourakos & Vourlidas (2009). Second, we observed the prominence/filament oscillations. Since they are located low in the corona, we can derive the velocity of the shocks/waves there from the distances and the times of the oscillations. In the current case, we need waves with velocities of 570 km s^{-1} or more. The direction of the filament is close to Line 3, and the required velocity is much faster than the slow-bright wave (S3b), while it is consistent with the fast-faint wave (F3f).

We thank the referee for the useful comments. This work is supported by KAKENHI (23340045) and by the Global COE Program "The Next Generation of Physics, Spun from Universality and Emergence" from MEXT, Japan.

REFERENCES

Asai, A., Hara, H., Watanabe, T., et al. 2008, ApJ, 685, 622
Chen, P. F., Fang, C., & Shibata, K. 2005, ApJ, 622, 1202
Chen, P. F., Wu, S. T., Shibata, K., & Fang, C. 2002, ApJ, 572, L99
Chen, P. F., & Wu, Y. 2011, ApJ, 732, L20
Delannée, C., & Aulanier, G. 1999, Sol. Phys., 190, 107
Eto, S., Isobe, H., Narukage, N., et al. 2002, PASJ, 54, 481
Gallagher, P. T., & Long, D. M. 2010, Space Sci. Rev., 158, 365
Harra, L. K., Sterling, A. C., Gömöry, P., & Veronig, A. 2011, ApJ, 737, L4
Hershaw, J., Foullon, C., Nakariakov, V. M., & Verwichte, E. 2011, A&A, 531, A53
Howard, R. A., Moses, J. D., Vourlidas, A., et al. 2008, Space Sci. Rev., 136, 67
Kai, K. 1970, Sol. Phys., 11, 310
Kaiser, M. L., Kucera, T. A., Davila, J. M., et al. 2008, Space Sci. Rev., 163, 5
Khan, J. I., & Aurass, H. 2002, A&A, 383, 1018
Khan, J. I., & Hudson, H. S. 2000, Geophys. Res. Lett., 27, 1083
Klassen, A., Aurass, H., Mann, G., & Thompson, B. J. 2000, A&AS, 141, 357
Kondo, T., Isobe, T., Igi, S., Watari, S., & Tokumaru, M. 1995, J. Commun. Res. Lab., 42, 111
Lemen, J. R., Title, A. M., Akin, D. J., et al. 2011, Sol. Phys.
Liu, W., Nitta, N. V., Schrijver, C. J., Title, A. M., & Tarbell, T. D. 2010, ApJ, 723, L53
Ma, S., Raymond, J. C., Golub, L., et al. 2011, ApJ, 738, 160
Mann, G., Jansen, F., MacDowall, R. J., Kaiser, M. L., & Stone, R. G. 1999, A&A, 348, 614
Moreton, G. E. 1960, AJ, 65, 494
Narukage, N., Hudson, H. S., Morimoto, T., et al. 2002, ApJ, 572, L109
Narukage, N., Ishii, T. T., Nagata, S., et al. 2008, ApJ, 684, L45
Narukage, N., Morimoto, T., Kadota, M., et al. 2004, PASJ, 56, L5
Newkirk, G., Jr. 1961, ApJ, 133, 983
Okamoto, T. J., Nakai, H., Keiyama, A., et al. 2004, ApJ, 608, 1124
Patsourakos, S., & Vourlidas, A. 2009, ApJ, 700, L182
Shibata, K., Kitai, R., Katoda, M., et al. 2011, Solar Activity in 1992–2003 (Kyoto: Kyoto Univ. Press)
Shiota, D., Kusano, K., Miyoshi, T., Nishikawa, N., & Shibata, K. 2008, J. Geophys. Res., 113, A03S05
Smith, S. F., & Harvey, K. L. 1971, in Physics of the Solar Corona, ed. C. J. Macris (Dordrecht: Reidel), 156
Thompson, B. J., Gurman, J. B., Neupert, W. M., et al. 1999, ApJ, 517, L151
Thompson, B. J., & Myers, D. C. 2009, ApJS, 183, 225
Thompson, B. J., Reynolds, B., Aurass, H., et al. 2000, Sol. Phys., 193, 161
Title, A., & AIA Team. 2006, BAAS, 38, 261
Tripathi, D., Isobe, H., & Jain, R. 2009, Space Sci. Rev., 149, 283
Uchida, Y. 1968, Sol. Phys., 4, 30
UeNo, S., Nagata, S., Kitai, R., Kurokawa, H., & Ichimoto, K. 2004, Proc. SPIE, 5492, 958
Veronig, A. M., Temmer, M., & Vršnak, B. 2008, ApJ, 681, L113
Warmuth, A. 2007, in The High Energy Solar Corona: Waves, Eruptions, Particles, ed. K. L. Klein & A. L. Mackinnon (Lecture Notes in Physics, Vol. 725; Berlin: Springer), 107
Warmuth, A., & Mann, G. 2011, A&A, 532, 151
Warmuth, A., Vršnak, B., Magdalenić, J., Hanslmeier, A., & Otruba, W. 2004a, A&A, 418, 1101
Warmuth, A., Vršnak, B., Magdalenić, J., Hanslmeier, A., & Otruba, W. 2004b, A&A, 418, 1117
Wills-Davey, M. J., & Attrill, G. D. R. 2009, Space Sci. Rev., 149, 325